J|A|C|S
ARTICLES
Published on Web 11/21/2002

Dimensional Changes as a Function of Charge Injection in Single-Walled Carbon Nanotubes

Guangyu Sun,[†] Jenö Kürti,[†,‡] Miklos Kertesz,*[,†] and Ray H. Baughman[§]

Contribution from the Department of Chemistry, Georgetown University, Washington, DC 20057, Department of Biological Physics, Eötvös University, Budapest, Hungary, and Department of Chemistry and NanoTech Institute, University of Texas at Dallas, Richardson, Texas 75083

Received April 29, 2002

Abstract: Motivated by the central importance of charge-induced dimensional changes for carbon nanotube electromechanical actuators, we here predict changes in nanotube length and diameter as a function of charge injection for armchair and zigzag nanotubes having different diameters. Density functional theory with periodic boundary conditions is used, which we show provides results consistent with experimental observations for intercalated graphites. Strain-versus-charge relationships are predicted from dimensional changes calculated with a uniform background charge ("jellium") for representing the counterions. These jellium calculations are consistent with presented calculations that include specific counterions for intercalated graphite, showing that hybridization between the ions and the graphite sheets is unimportant. The charge−strain relationships calculated with the jellium approximation for graphite and isolated single-walled nanotubes are asymmetric with respect to the sign of charge transfer. The dependence of nanotube strain on charge approaches that for a graphite sheet for intermediate-sized metallic nanotubes and for larger diameter semiconducting nanotubes. However, the strain−charge curves strongly depend on nanotube type when the nanotube diameter is small. This reflects both the dependence of the frontier orbitals for the semiconducting nanotubes on the nanotube type and the $\pi-\sigma$ mixing when the nanotube diameter is small.

Introduction

Polymeric π-bonded materials such as *trans*-polyacetylene, graphite, and single-walled carbon nanotubes (SWNTs) undergo dimensional changes as a consequence of either chemical or electrochemical doping.[1] The magnitude of the dimensional changes depends on the amount and sign of the charge transferred to carbon, q, which is negative for donor dopants (such as alkali metals) and positive for acceptor dopants (such as halogens). It has been experimentally shown for doped *trans*-polyacetylene[2−3] and graphite[4] that charge transfer causes asymmetrical changes in the dimension of the covalent network: negative charge injection causes expansion and positive charge injection causes contraction. The asymmetry of the sign of strain for the covalent networks[5] (S) with respect to the sign of q is a key feature studied in this paper. Shrinkage of the average C−C bond length upon acceptor doping is counterintuitive and is quantum mechanical in origin. On the other hand, expansion occurs in the van der Waals bonded direction perpendicular to the C−C network when donor or acceptor ions larger than unsolvated lithium are intercalated, and this effect is attributed to the occupied volume of the intercalated ion. Strain caused by either the volume of intercalated ions or bond length changes as a result of charge transfer have been proposed for electrochemical actuation of conjugated polymers.[6] An "artificial muscle" using these covalent bond length changes (which are essentially independent of ion size effects) has been recently demonstrated with electrochemical double-layer charging of sheets made of bundles of SWNTs.[7]

Earlier theoretical studies[1,8−10] have assumed the existence of a generic (non-counterion-specific) charge−strain relationship for the carbon network. Several mechanisms have been proposed to explain the observed asymmetry of the charge−strain curves. The frontier orbitals of both *trans*-polyacetylene and graphene are nonbonding but display antibonding characteristics for second-neighbor carbon atoms. This weak antibonding interaction of the delocalized π-orbitals around the Fermi level was

* Corresponding author: e-mail kertesz@georgetown.edu.
[†] Georgetown University.
[‡] Eötvös University.
[§] University of Texas at Dallas.

(1) (a) Kertesz, M.; Vonderviszt, F.; Hoffmann, R. In *Intercalated Graphites*; Dresselhaus, M. S., Dresselhaus, G., Fischer, J. E., Moran, M. J., Eds.; Elsevier: Amsterdam, 1983; p 141. (b) Kertesz, M. *Mol. Cryst. Liq. Cryst.* **1985**, *126*, 103.
(2) Murthy, N. S.; Miller, G. G.; Baughman, R. H. *J. Chem. Phys.* **1988**, *89*, 2523.
(3) Winokur, M. J.; Moon, Y. B.; Heeger, A. J.; Barker, J.; Bott, D. C. *Solid State Commun.* **1988**, *68*, 1055.
(4) Hérold, A. In *Intercalated Layered Materials*: Levy, F., Ed.; D. Reidel Publishing: Dordrecht, Boston, and London, 1979; p 321.
(5) Strain is defined as the percentage change of the lattice constant(s) along the dimension(s) containing the C−C bonds, $S(q)$ for a given charge per carbon, q.
(6) Baughman, R. H. *Synth. Met.* **1996**, *78*, 339.
(7) Baughman, R. H.; Cui, C.; Zakhidov, A. A.; Iqbal, Z.; Barisci, J. N.; Spinks, G. M.; Wallace, G. G.; Mazzoldi, A.; Rossi, D. D.; Rinzler, A. G.; Jaschinski, O.; Roth, S.; Kertesz, M. *Science* **1999**, *284*, 1340.
(8) (a) Hong, S. Y.; Kertesz, M. *Phys. Rev. Lett.* **1990**, *64*, 3031. (b) Kertesz, M.; Vonderviszt, F.; Pekker, S. *Chem. Phys. Lett.* **1982**, *90*, 430.
(9) Chan, C. T.; Kamitakahara, W. A.; Ho, K. M.; Eklund, P. C. *Phys. Rev. Lett.* **1987**, *58*, 1528.
(10) Pietronero, L.; Strässler, S. *Phys. Rev. Lett.* **1981**, *47*, 593.

10.1021/ja020616j CCC: $22.00

shown to correlate well with this asymmetry in the case of doped *trans*-polyacetylene and graphite.[1,8] An earlier density functional theory calculation for graphite also displays this asymmetry,[9] which results from the change of the charge density of the σ bond. An alternative model based on the change of the effective atomic potential due to the extra charge has been used in a tight-binding study for intercalated graphite compounds.[10] In these earlier charge−strain calculations, the possible modifying effects of specific counterions, like the hybridization between the counterions and the carbon network, were not included.

Since recent experimental results[7] show the potentially high performance of carbon nanotube actuators, more detailed understanding of the charge−strain relationships of carbon-based π-bonded materials is of interest. Better understanding of the strain caused by charge transfer is needed in order to interpret the electrochemical actuation of SWNTs and to guide optimization of actuation. In this work, density functional theory is used to predict and analyze the $S(q)$ curves (strain S as a function of charge q) of isolated SWNTs having different geometries. For comparison and to test the reliability of the theoretical approach, the strains caused by charge transfer in intercalated graphite are also calculated and compared with experimental results.

Computational Method

Geometry optimizations for graphite and SWNTs used density functional theory and the generalized gradient approximation (GGA). The Perdew−Wang 91 (PW91)[11] GGA functional was used in combination with ultrasoft Vanderbilt-type pseudopotentials[12] generated for the PW91 exchange-correlation functional. Calculations were performed with the Vienna ab initio simulation package (VASP v.4.4.2), which is a plane-wave, solid-state program.[13,14] Default cutoff energies designated as "medium accuracy" were used, e.g., 290 eV for carbon. The VASP code has been shown to produce reliable structures for various organic molecules, including conjugated molecules and molecular ions,[15] graphite and diamond,[16] and SWNTs.[17] The VASP program was modified to allow relaxation of the unit cell and the atomic positions in selected dimensions. Convergency was enhanced by use of fractional occupancy by Gaussian broadening ($\sigma = 0.10$ eV) of the one-electron energy levels. Monkhorst−Pack-type k-point meshes having the origin at the Γ-point were used. Figure 1 illustrates the unit cells utilized for the single-walled carbon nanotubes and intercalated graphites.

Two types of calculations were carried out to simulate the graphite intercalation compounds and SWNTs. In the full calculations, the intercalated graphite structures for XC_6 (X = Li, Ca, and Ba), KC_8, and acceptor compounds C_6Cl, $C_{18}PF_6$, and $C_{24}AsF_6$ were optimized. C_6Cl is a hypothetical compound, which we included in our modeling only to establish the consistency of our approach and provide further support for the generic $S(q)$ curves for intercalated graphites. The counterion was always located midway between two adjacent graphene layers and above the center of a six-membered ring. The orientations of polyatomic anions (PF_6 and AsF_6) were not optimized. Otherwise, all geometrical parameters were relaxed in these calculations. The amounts of electron transfer were estimated by numerically integrating the electronic states that are filled or emptied around the Fermi level with the rigid-band model.

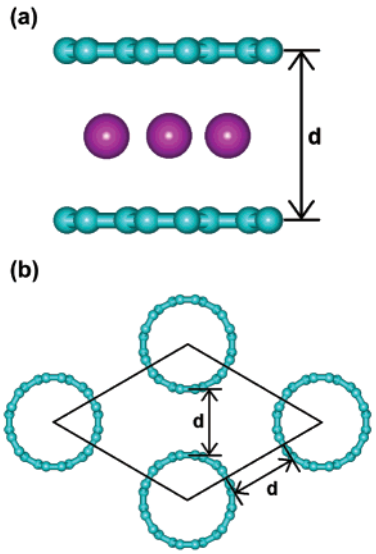

Figure 1. Unit cells used in this study for (a) graphite intercalation compounds and (b) single-walled carbon nanotubes.

We used the 18 × 18 × 12 k-point set for atomically doped graphites, while for the AsF_6- and PF_6-doped graphites we used the 8 × 8 × 4 set. For the undoped hexagonal graphite we used a 30 × 30 × 10 set. For the nanotube calculations the k-point mesh varied from 1 × 1 × 30 for small-diameter nanotubes to 1 × 1 × 24 (armchair) and 1 × 1 × 20 (zigzag) for the medium to 1 × 1 × 12 for the largest ones.

Charge−strain curves were also produced that are generic in the sense that they are not ion-specific. Only the atoms of graphite or nanotubes were included in these generic calculations and the counterions were represented by a uniform background charge (jellium). The additional charge on the carbon networks was introduced by filling the lowest unoccupied orbitals or emptying the highest occupied orbitals. The uniformly distributed background charge with opposite sign was used in order to compensate the charge on the carbon network. An intertube and intersheet distance of $d = 6$ Å was used for the jellium calculations for graphite (Figure 1a) and the isolated SWNTs (Figure 1b). Use of d values between 4 and 10 Å changes the predicted expansion coefficients (strain in percent per charge per carbon) for graphite at near zero charge by less than 20%.[18] However, the charge−strain curves increasingly depend on the choice of d for increasing amount of injected charge, since electrostatic terms become progressively more important as the amount of donated charge increases.

Graphite Intercalation Compounds

The in-plane strain has been experimentally derived for graphite intercalation compounds by comparing the a-axis dimension measured by X-ray diffraction for intercalated and nonintercalated graphite.[19−24] Figure 2 shows these experimental data taken from the literature. On the negative charge side, the experimental data are consistent with roughly monotonic expansion of the in-plane graphite dimension on adding up to about 0.2 electron/carbon (a charge of −0.2e in our convention), and perhaps as much as 0.3 electron/carbon (which is the limit of

(11) Perdew, J. P.; Wang, Y. *Phys. Rev. B* **1992**, *45*, 13244.
(12) Vanderbilt, D. *Phys. Rev. B* **1990**, *41*, 7892.
(13) Kresse, G.; Furthmüller, J. *Phys. Rev. B* **1996**, *54*, 11169.
(14) Kresse, G.; Hafner, J. *Phys. Rev. B* **1993**, *47*, R558.
(15) Sun, G. Y.; Kürti, J.; Rajczy, P.; Kertesz, M.; Hafner, J.; Kresse, G. *J. Mol. Struct. THEOCHEM*, accepted.
(16) Kresse, G.; Furthmüller J.; Hafner, J. *Europhys. Lett.* **1995**, *32*, 729.
(17) (a) Kürti, J.; Kresse, G.; Kuzmany, H. *Phys. Rev. B* **1998**, *58*, 8869. (b) Milnera, M.; Kürti, J.; Hulman, M.; Kuzmany, H. *Phys. Rev. Lett.* **2000**, *84*, 1324.
(18) Sun, G. Y. Ph.D. Thesis, Georgetown University, Washington, DC, 2002.
(19) Nixon, D. E.; Parry, G. S. *J. Phys. C Solid State* **1969**, *2*, 1732.
(20) Fischer, J. E.; Kim, H. J.; Cajipe, V. B *Phys. Rev. B* **1987**, *36*, 4449.
(21) Baron, F.; Flandrois, S.; Hauw, C.; Gaultier, J. *Solid State Commun.* **1982**, *42*, 759.
(22) Flandrois, S.; Masson, J. M.; Rouillon, J. C.; Gaultier, J.; Hauw, C. *Synth. Met.* **1981**, *3*, 1.
(23) Markiewicz, R. S.; Kasper, J. S.; Interrante, V. *Synth. Met.* **1980**, *2*, 363.
(24) Murakami, Y.; Kishimoto, T.; Suematsu, H. *J. Phys. Soc. Jpn.* **1990**, *59*, 571.

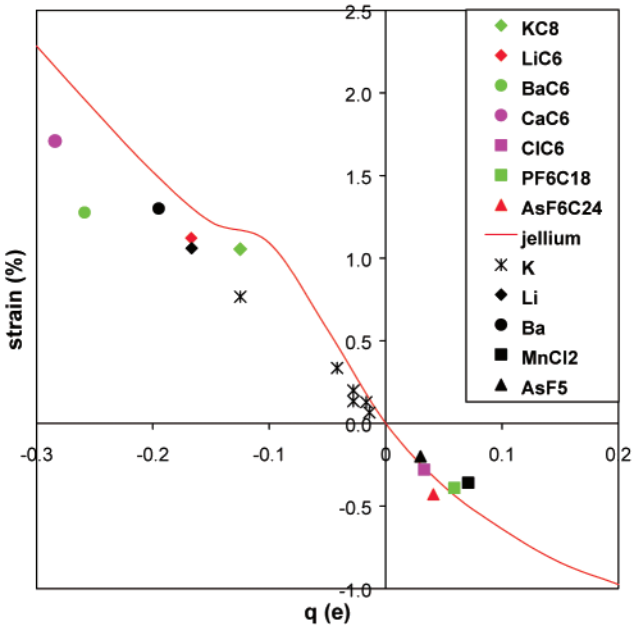

Figure 2. Theoretical strain in graphite intercalation compounds and charged graphene as calculated by density functional theory. Marks in color represent theoretical results; the red solid line represents the generic curve. Experimental data for intercalated graphite compounds are also shown in black for comparison. The doping agents are indicated in the inset; the references to the experimental work are as follows. K, ref 19; Li, ref 25; Ba, ref 20; $MnCl_2$, ref 21; AsF_5, ref 23.

the experimentally derived data). The experimentally accessible charge range is much smaller on the positive charge side, and the available experimental data scatter in a narrow region.

The theoretical calculations shown in Figure 2 are of two types. Full calculations including the specific counterions constitute the first type. The considered graphite intercalation compounds in Figure 2 involve the donors Li, K, Ca, and Ba and the acceptors Cl, PF_6, and AsF_6. For the donor-doped graphites where experimental strain values are available, the agreement with experiment is excellent. Charge transfer is nearly complete for Li- and K-doped graphite, providing close to 1 electron/dopant ion. For Ca- and Ba-doped graphite, the charge transfer per dopant atom is estimated theoretically as 1.7 and 1.6 electrons, respectively. An earlier experimental study[25] estimated the charge transfer in BaC_6 to be above 0.8 electron/dopant ion; the more recent estimate[20] of 1.17 e/barium yields $q = 0.195$ e/carbon. Among the acceptor dopants, the charge transfer for the hypothetical Cl-doped graphite is estimated theoretically to be only 0.23 electron/chlorine. Due to the large electron affinity of fluorine, the charge transfers for PF_6- and AsF_6-doped graphite are theoretically estimated to be complete, resulting in a per-carbon electron charge of $q = {}^1/_{18}$e and ${}^1/_{24}$e, respectively.

The second type of calculation is the generic jellium calculation. The continuous jellium calculation curve for $d = 6$ Å predicts that negative charge causes expansion of the in-plane lattice and positive charge causes contraction (as long as the amount of charge injection is not too large). The main features of the generic $S(q)$ curve of graphite are in agreement with the experimental data for the graphite intercalation compounds. The kink around $q = -0.1$e in the generic curve is a consequence of the vicinity of σ^* and π^* bands. The change in the slope is related to the different bonding characteristics of the π^* and σ^* orbitals involved in the charge transfer. Earlier theoretical

Table 1. Comparison of the Interlayer Distances in Graphite Intercalation Compounds Calculated by Density Functional Theory (VASP) and Experiment

	theory	exp (Å)		theory	exp (Å)
LiC_6	3.48	3.706[a]	C_6Cl	5.57	NA
KC_8	5.35	5.32−5.41[b]	$C_{18}PF_6$	7.74	7.95[c]
CaC_6	4.49	4.60[d]	$C_{24}AsF_6$	7.37	7.6[e]
BaC_6	5.46	5.25[f]	graphite	3.393	3.35[g]

[a] Taken from ref 25. [b] Taken from ref 26. [c] Taken from ref 29. Experimental composition approximately corresponds to C_{24}^+ per dopant. [d] Taken from ref 27. [e] Taken from ref 30. Experimental value corresponds to the composition of $C_{14}AsF_6$. [f] Taken from ref 28. [g] Taken from ref 4 for hexagonal graphite, p 327.

studies[1,9,10] also predicted the asymmetry of graphite in-plane strain as a function of the direction of charge transfer. Quantitatively, the strain in our curve is smaller than that of Pietronero and Strässler[10] but larger than that of Kertesz et al.[1] and Chan et al.[9] Kertesz et al.[1] obtained a linear term in the $S(q)$ curves due to the second-neighbor antibonding interactions present in their semiempirical calculations. These interactions break the electron−hole symmetry. Pietronero and Strässler introduced a semiempirical model, in which the Coulomb interactions changed linearly with the atomic charges, leading to the experimentally observed linear term in the $S(q)$ curve for graphite. The present calculations and the calculations of Chan et al.[9] are ab initio and include both effects.

The calculated CC bond distance in undoped graphite is 1.419 Å, which is in excellent agreement with the experimental value of 1.42 Å (ref 4, page 329). In addition to finding support in the good agreement between the calculated and experimental values of in-plane strain as a function of charge injection, the calculation method is supported by the agreement between experimental[26−31] and predicted interlayer distances for various graphite intercalation compounds. Table 1 compiles the optimized interlayer distances and compares them with the reported experimental values for the graphite intercalation compounds and undoped graphite. Note that comparison for the acceptor-doped graphite compounds is qualitative because the structures of these compounds have not been fully characterized.

As will be described later, the similarly predicted generic $S(q)$ curve for *trans*-polyacetylene agrees well with both the available experimental data and the result of full calculations that include specific counterions.[32] In fact, the $S(q)$ curves for graphite sheets and *trans*-polyacetylene chains are quite similar.

Single-Walled Carbon Nanotubes

The structures of single-walled carbon nanotubes can be generated by wrapping a suitably cut ribbonlike segment of an infinite graphene sheet along a roll-up vector (n, m).[33] According to Hückel (or tight binding) theory, SWNTs have a nonzero band gap and are semiconducting unless $(n - m)/3$ is an integer,

(25) Preil, M. E.; Fischer, J. E.; Dicenzo, S. B.; Wertheim, G. K. *Phys. Rev. B* **1984**, *30*, 3536.
(26) (a) Juza, R.; Wehle, V. *Naturwissenschaften* **1965**, *52*, 560. (b) Guérard, D.; Hérold, A. *Carbon* **1975**, *13*, 337.
(27) (a) Rüdorff, W.; Schultze, E. *Z. Anorg. Allg. Chem.* **1954**, *277*, 156. (b) Billaud, D.; Hérold, A. *Bull. Soc. Chim. Fr.* **1971**, 103. (c) *Ibid.* **1974**, 2042. (d) *Ibid.* **1974**, 2407.
(28) Guérard, D.; Hérold, A. *C. R. Seances Acad. Sci., Ser. C* **1975**, *280*, 729.
(29) Guérard, D.; Hérold, A. *C. R. Seances Acad. Sci., Ser. C* **1974**, *279*, 445.
(30) Zhang, Z.; Lerner, M. M. *J. Electrochem. Soc.* **1993**, *140*, 742.
(31) Okino, F.; Bartlett, N. *J. Chem. Soc., Dalton Trans.* **1993**, 2081.
(32) (a) Sun, G. Y.; Kertesz, M.; Kurti J.; Baughman, R. H. *Polym. Mater. Sci. Eng.* **2000**, *83*, 519. (b) Sun, G. Y.; Kürti, J.; Kertesz, M.; Baughman, R. H. *J. Chem. Phys.* **2002**, *117*, 7691.

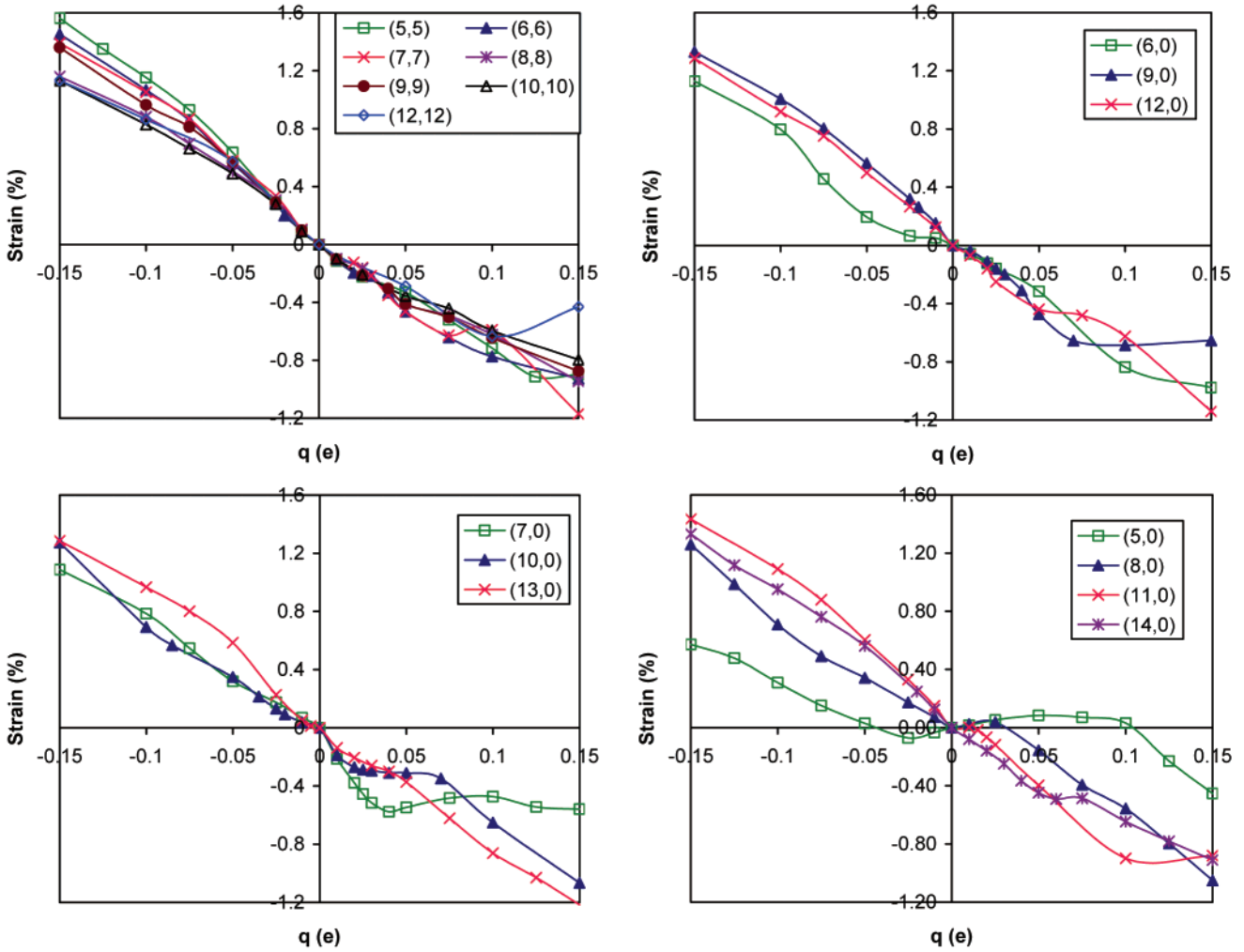

Figure 3. Theoretical strain response of armchair (n, n) (a, upper left) and three series of zigzag (n, 0) single-walled carbon nanotubes: (b, upper right) $n = 3i$; (c, lower left) $n = 3i + 1$; (d, lower right) $n = 3i + 2$.

in which case they are metallic.[33] Although the three-dimensional structures of SWNTs are different from that of graphene (a sheet of graphite), their covalent connectivities and bonding are very similar. This leads to the expectation that the $S(q)$ curves for SWNTs should be similar to those of graphene, at least when the nanotube radius is large. The largest differences between $S(q)$ for graphite and carbon nanotubes are expected to occur for small-radius semiconducting nanotubes.

All (n, n) "armchair" tubes are metallic at the Hückel level of theory. This is in agreement with our density functional theory result. The predicted $S(q)$ curves for armchair SWNTs from (5, 5) to (12, 12) are shown in Figure 3a. All these curves closely resemble each other and that of graphene.

The "zigzag" (n, 0) nanotubes are predicted at the Hückel theory level to be metallic or nearly metallic when n is a multiple of 3 and semiconducting otherwise.[33] In our density functional theory results, zigzag nanotubes with $n > 7$ follow this prediction. Zigzag nanotubes with $n \leq 7$ have small or zero band gaps due to their small radius and correspondingly significant $\sigma-\pi$ mixing.[34] The predicted band gaps are 0.5−1 eV for the semiconducting tubes when $n > 7$.

Panels b−d of Figure 3 show the $S(q)$ curves obtained from the jellium calculations for zigzag SWNTs. Different behavior is predicted for nanotubes with $n = 3i$, $3i + 1$, and $3i + 2$, where i is an integer. For zigzag nanotubes with $n = 3i$, the predicted $S(q)$ generally agrees with that of graphene and armchair SWNTs. Noticeable deviation, however, is seen for nanotubes of this type that are as small in diameter as a (6, 0) nanotube, where the calculated strain values are significantly reduced relative to those of graphene in the $-0.1e < q < 0$ range. Also, some deviations exist between calculated results for the (6, 0), (9, 0), and (12, 0) nanotubes for positive values of injected charge.

For the $n = 3i + 1$ series, the $S(q)$ curves initially take a deep dive (a contraction) upon initial addition of positive charge and then turn back up and approach the graphene curve, except for the (7, 0) case, where the nanotube diameter is particularly small. This deviation from graphene behavior diminishes with increasing tube radius. On the negative q side, the strain curves for all but the smallest diameter nanotube are similar to that of graphene.

For the $n = 3i + 2$ series, there is considerable variation in $S(q)$, especially for $n \leq 11$. For small values of positive charge, even the sign of the strain differs from the case where n belongs to either of the other two series: small positive strain is predicted

(33) Saito, R.; Dresselhaus, G.; Dresselhaus, M. S. In *Physical properties of carbon nanotubes*; Imperial College Press: London, 1998; p 35.
(34) Blase, X.; Benedict, L. X.; Shirley, E. L.; Louie, S. G. *Phys. Rev. Lett.* **1994**, *72*, 1878.

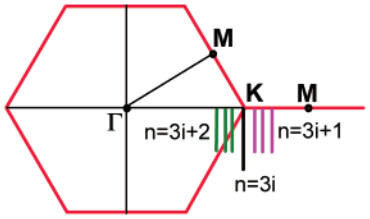

Figure 4. Locations of the *k*-points corresponding to the highest occupied and lowest unoccupied orbitals for the three types of zigzag (*n*, 0) nanotubes are mapped on the two-dimensional *k*-space of graphene. When n increases, these *k*-points approach the *K* point along the *MK* line for the $n = 3i + 1$ series and the Γ*K* line for the $3i + 2$ series.

for $n = 5$ and 8 when small amounts of positive charge are injected into the nanotube. For the $n = 11$ intermediate case, the strain associated with charge injection is close to zero for $0 < q < 0.02$e. On the negative q side, the strain is negative for the (5, 0) nanotube when charge is small and changes to a positive strain when the amount of injected negative charge exceeds −0.04e. The curve for $n = 8$ is below that of graphene on the negative side, whereas the curve for $n = 11$ resembles that of graphene. For the larger nanotube with $n = 14$, the entire $S(q)$ curve resembles that of graphene with minor deviation.

The radii of the nanotubes also depend on the amount of injected charge per carbon (see Supporting Information, Figures S1 and S2). However, the calculated strains in the radial direction dramatically differ from the strains in the direction of tube axis and can have opposite signs. Hence, charge-induced changes in nanotube dimensions occur highly anisotropically, at least until the nanotube radius becomes large. In this large radius limit, this anisotropy is expected to disappear, since the charge-induced expansions in both radial and tube direction should approach that of graphite sheet.

The charge-induced strain of armchair and zigzag SWNTs is predicted to be similar to that of graphene for nanotubes with sufficiently large radii, regardless of whether the tubes are metallic. For nanotubes with small radii, various charge−strain curves are predicted due to the different electronic band structures for different nanotubes. The strain−charge behavior is sensitive to the bonding/antibonding characteristics of the orbitals that are involved in the charge-transfer process. Approximate band structures for nanotubes can be generated from that of graphene by limiting the energy levels to a set of allowed *k*-points determined by the *n* and *m* values of the roll-up vector.[33] In Figure 4, the hexagon is the first Brillouin zone of graphene. The allowed *k*-points of SWNTs can be mapped onto the Brillouin zone of graphene as described in ref 33. The *k*-points corresponding to the highest occupied and lowest unoccupied levels of nanotubes are those closest to the *K* point in the two-dimensional band structure of graphene. The orbitals around this particular *K* point have been shown to have second-neighbor antibonding character.[1]

For the armchair nanotubes, the allowed *k*-points corresponding to the highest occupied and lowest unoccupied levels go through the *K* point, where π and π^* bands of graphene meet. Therefore the highest occupied and lowest unoccupied orbitals are similar to that of graphene, and thus similar strain behavior to that of graphene is expected. The allowed *k*-points corresponding to the highest occupied and lowest unoccupied orbicals for the zigzag nanotubes are illustrated in Figure 4. The allowed *k*-points of the $n = 3i$ series include the *K* point. For the two other series, $n = 3i + 1$ and $3i + 2$, these *k*-points approach the *K* point along the *MK* and Γ*K* lines, respectively, as *n* increases. Since the bonding characteristics of the orbitals corresponding to the energy levels along the *MK* and Γ*K* lines are different, different $S(q)$ curves are expected for these two series of nanotubes. For large-radius nanotubes, these *k*-points are closer to the *K* point and as a result, strain−charge behavior similar to that of graphene is obtained.

Conclusions

Density functional theory has been used to successfully predict the observed strains resulting from charge injection in graphite intercalation compounds and to predict the charge-induced strain for selected isolated carbon SWNTs. The calculated charge−strain curves are generic since they are independent of the specific counterion and whether the counterions are intercalated or present in a double layer. This approach has the greatest reliability when the amount of charge injection is small, since structure-specific variations in electrostatic effects are quadratic in charge. By use of the generic charge−strain curves, armchair nanotubes are predicted to provide similar dimensional behavior upon charge injection, as does graphite. Different charge−strain curves are predicted for zigzag (*n*, 0) nanotubes with $n = 3i$, $3i + 1$, and $3i + 2$, especially for nanotubes having small radii. These variations in behavior result from the different bonding behavior of the orbitals active in the charge-transfer process. Strain values resulting from calculations that explicitly include counterions agree very well with the generic calculations for graphite. Hence, we conclude that hybridization between particular counterions and the carbon network plays a relatively minor role in determining the strain response to charge transfer. Thus, in the regime where coulomb repulsion effects do not dominate, the generic $S(q)$ curves can be used to estimate the amount of charge transfer from a known value of charge-induced strain.

The key result of these studies is the establishment and validation of the generic charge−strain relationships for carbon networks including nanotubes. Future work will extend these studies to nanotubes with larger radii and nanotubes with heteroatomic substitutions in order to attempt to maximize the predicted actuation response per unit charge transferred.

Acknowledgment. Financial support from the National Science Foundation (Grants CHEM-9802300 and CHEM-9601976) and from Defense Advanced Research Projects Agency (Grants N00173-99-2000 and MDA 972-02-C-0005) is gratefully acknowledged. Work in Hungary was supported by Grants FKFP-0144/2000 and OTKA-T038014. We thank Professor Amy Liu (Department of Physics, Georgetown University) and three anonymous referees for their constructive comments. Partial support to R.H.B. by the Robert A. Welch Foundation is gratefully acknowledged.

Supporting Information Available: Two figures showing theoretical percentage change of the radii of response of armchair and zigzag single-walled carbon nanotubes. This information is available free of charge via the Internet at http://pubs.acs.org.

JA020616J